

Pattern selection and regulation using noise in a liquid metal

Pawan Kumar, J. M. Cruz, and P. Parmananda

Department of Physics, Indian Institute of Technology Bombay, Powai, Mumbai-400 076, India

(Received 28 November 2018; published 22 April 2019)

Electric forcing can be used to select and to regulate the shape of liquid metals. In this work, we present a transition among different patterns in a liquid mercury drop regulated by noise. A stochastic resonancelike phenomenon was observed for two different structural transitions of the liquid metal. In the first set of experiments, the transition from irregular (I) \rightarrow triangular (T) \rightarrow irregular (I) patterns was obtained by increasing the amplitude of biased white noise. In the second part, we observed the transition from irregular (I) \rightarrow elliptical (E) \rightarrow irregular (I) patterns using the same kind of noise. Periodic stochastic resonance was corroborated in our experiments by employing the cross-correlation coefficient technique.

DOI: [10.1103/PhysRevE.99.040201](https://doi.org/10.1103/PhysRevE.99.040201)**I. INTRODUCTION**

Liquid metals have low viscosity, high conductivity, stretchability, and surface reconfigurable properties [1]. Due to their unique features, liquid metals have a wide range of applications in soft robotics, stretchable electronics, e-skin, and wearables [1–3]. The regulation of liquid metals has focused mainly on the study of changing their shape and position under the influence of applied ac [4–6] and dc [7–9] potentials. In the last few years, the rich dynamical behavior and the potential technological applications of liquid metals have attracted the attention of the scientific community.

Mercury (Hg), gallium (Ga), and Ga alloys are suitable liquid metals for many practical uses. In particular, Hg⁰ has diverse applications such as diffusion pumps, measuring instruments (barometers, thermometers), and as an electrode in polarography [1]. In 1858, Kühne discovered the mercury beating heart (MBH) system while the first report was made by Lippmann in 1873 [10]. The MBH system simultaneously exhibits chemical and mechanical activities and shows a plethora of different dynamical topologies in both autonomous [10–13] and nonautonomous [5,6] configurations. In the autonomous MBH system, regular and irregular oscillations of electrical and mechanical activities have been reported [11–13]. The nonautonomous system has also been studied in various experimental scenarios such as the variation of topological shapes via forcing frequency [5,14] and amplitude [14], rotational motion of mercury drop, traveling waves [8], standing waves [15], control of aperiodic oscillations [16], and synchronization of two forced MBH oscillators [17].

In day-to-day life noise plays an essential role. Not long ago it was thought that noise was only a nuisance, hindering the information and transformation of signals. However, noise does not play a destructive role only [18–20]; there are evidences in natural and laboratory systems where noise has a positive contribution [21–25]. Some demonstrations of this constructive role are synchronization of uncoupled oscillators [26–28], stochastic resonance (SR) [21–25,29–36], and coherence resonance [37–40].

In particular, stochastic resonance refers to a mechanism in which a stochastic signal enhances the performance of a

weakly driven nonlinear system. The term stochastic resonance was conceived by Benzi *et al.* to explain the periodic recurrence of glacial and interglacial stages [21,22]. The first evidence of SR in a laboratory was made by Fauve and Heslot using a Schmitt trigger oscillator [41]. Later, McNamara *et al.* reported the observation of SR in a bidirectional ring laser [42]. Nowadays, the study of SR covers a wide range of research areas from the macroscopic to the microscopic level, e.g., SR was found in mechanoreceptor neurons located in the tail fan of crayfish [30] and hair cells of crickets [43]. In the field of nonlinear dynamics, SR has been extended from coupled oscillators [31,44–46] to spatiotemporal systems [47]. Stochastic resonance has been explored using various types of noise such as white noise (zero-mean) [22,41], colored noise [48], multiplicative noise [49], and white noise with different mean intensity [43]. Moreover, the use of biased noise has been very successful to obtain logic gates, which is a relevant application of SR named logical stochastic resonance [50,51]. All these significant studies of the SR mechanism support many practical applications in different areas of science and technology [52,53].

In this work, the selection and regulation of a liquid metal pattern has been achieved using a biased white noise signal. In our experimental setup, without any external forcing, no oscillations occur on the liquid metal. In order to induce the oscillatory activities of the Hg drop, we applied a square-wave signal. To determine the transitions of the different shapes of the liquid metal, a systematic scan of the periodic forcing amplitude was performed, from 2.0 to 0.25 V. Further, to obtain the periodic stochastic resonance (PSR), a biased (nonzero distinct mean) white noise stimulus was superimposed to a subthreshold periodic signal. The experiments to study the PSR have been distributed over two sets in this Rapid Communication. The protocol in both sets is such that, on applying the subthreshold square-wave potential, without noise, the liquid metal drop exhibited irregular shape oscillations. Thereafter, in the first set of experiments (Sec. III A), positive bias noise amplitude (from 1.6 to 0.5 V) regulated the transitions from irregular (I) \rightarrow triangular (T) \rightarrow irregular (I) and, in the second set of experiments (Sec. III B), negative bias noise

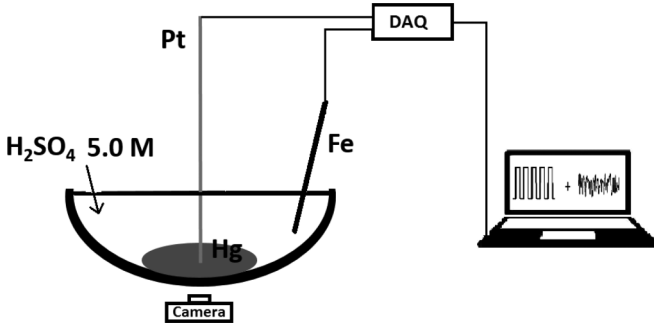


FIG. 1. Schematic diagram representing an MBH oscillator connected with the external DAQ control card. The Pt wire is immersed in the center of the Hg drop to provide electrical contact. The iron wire is dipped in the H_2SO_4 . The external signal is generated in the computer and applied across the Pt and Fe electrodes. H_2SO_4 5.0 M is the electrolytic solution.

amplitude (from -0.2 to -1.55 V) regulated the transitions from irregular (I) \rightarrow elliptical (E) \rightarrow irregular (I).

The different sections of our work are structured as follows. In Sec. II, we describe the experimental setup that was used. Our main results are presented in Sec. III and the Rapid Communication concludes with a discussion and summary in Sec. IV.

II. EXPERIMENTAL SETUP

The schematic diagram of the experimental setup configured to study the PSR in an MBH oscillator is shown in Fig. 1. The system consists of a concave watch glass with a radius of curvature of 7.56 cm containing 0.9 ml of Hg, 28 ml of sulfuric acid (H_2SO_4) 5.0 M (Merck, Emparta ACS, 98.0%) as the electrolyte, an iron (Fe) wire (Alfa Aesar, 2.0 mm diameter, > 99.0% purity), and a platinum (Pt) wire (Sigma-Aldrich, 0.5 mm diameter, 99.99% purity). Before conducting the experiments, the mercury was cleaned: we put 40 ml of Hg and 400 ml of H_2SO_4 1.0 M in stirring for 24 h. After that the mercury was rinsed three times with deionized water. The iron wire (polished with sandpaper No. 400 and No. 1000 before each experiment) was immersed in the electrolytic solution at the edge of the watch glass avoiding contact with the Hg drop. The Pt wire, free of impurities, was submerged in the center of the liquid metal providing electrical contact. The external forcing was generated in the computer and provided across the Fe and Pt electrodes using a data acquisition control card (DAQ measurement computing USB-1616HS-4, 1000 Hz). To record the mechanical activities of the MBH oscillator a Go-Pro Hero 4 camera was used. All videos have been recorded for the lapse time of 90 s. The normalized area (NA) time series were computed from the videos (the central cross-section area of the liquid metal drop was extracted using a MATLAB program; this protocol helps us to distinguish the mechanical activities at different amplitudes of noise). All the data has been extracted after the transients. So, the area time series has been extracted only for the last 50 s of each video. The experiments were performed at $25 \pm 1^\circ\text{C}$.

III. EXPERIMENTAL RESULTS

To regulate the patterns of the system, we used the superposition of a periodic square-wave signal and biased white noise, i.e., $V(t) = V_0(t) + D\eta(t)$, where $V_0(t)$ corresponds to the square-wave signal and “ $\xi(t) = D\eta(t)$ ” represents the white noise signal. Using the square-wave signal frequency (ν) and amplitude (A_f) of $V_0(t)$ the desired patterns were identified and selected to study the PSR phenomenon. To confirm the presence of the PSR, using the MATLAB interface inbuilt command `corrcoef[V0(t), NA]`, we computed the cross-correlation coefficient (CCC) between the input subthreshold periodic signal $V_0(t)$ and the output time series of the normalized area (mechanical activity, NA). The time-series span was the same for all data analysis of CCC values.


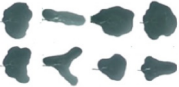

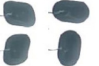


A. PSR: Irregular \rightarrow triangular \rightarrow irregular patterns

First, we performed a systematic scan of the periodic forcing amplitude A_f from 2.0 to 0.25 V, using $\nu = 7.90$ Hz. Table I shows the transitions from the different regimes of dynamical patterns. For values of A_f greater than 2.0 V, the pattern remains in the triangular shape. Thereafter, in order to find the PSR, we selected $A_f = 0.7$ V as the set point (for that value the liquid metal exhibited the irregular pattern) and then the biased white noise signal was superimposed on the system. The amplitude of the noise (D) was monotonically varied from 1.6 to 0.5 V.

Figure 2(I) shows the CCC plot exhibiting a unimodal profile, a hallmark of stochastic resonance. The domain for the higher values of CCC in the presence of the optimum noise represents the higher correlation between the input and the output signals. In this region, a regular pattern (oscillations exhibiting a triangular shape) of the Hg drop was achieved. For the higher and lower levels of noise intensity, CCC has lower values and the mechanical oscillations of the drop reveal irregular patterns.

Figure 2(II) shows five time series, wherein, the upper panel in blue (dark-gray) color represents the applied subthreshold square-wave signal and the lower panel in blue (dark-gray) color shows a biased white noise signal having $D = 1.0$ V. Figure 2(II) from (a) to (c), in orange (light-gray) color shows a section of the time series of the NA of the liquid metal under the influence of different amplitudes of white noise and the subthreshold square-wave signal. The section of the time series in panels (IIa), (IIb), and (IIc) displays the oscillations of the Hg drop corresponding to the points (a), (b), and (c) in Fig. 2(I). In this case, under the influence of noise, the triangular shape of the liquid metal drop loses its stability and becomes irregular at higher levels of noise amplitude, but using periodic forcing (Table I) the transition from irregular \rightarrow regular (triangular) was observed and even upon increasing the periodic forcing amplitude the triangular shape was sustained. To emphasize, the transitions with and without noise are not similar because, in one case, under the influence of noise, the triangular pattern is destroyed and on the other hand, using square-wave potential, the triangular pattern is preserved. Hence, the regulation of these patterns as a consequence of the noise is a fingerprint of the classical PSR phenomenon. The videos (Video1a, Video1b, and Video1c)

TABLE I. Systematic scan of A_f from 2.0 to 0.25 V, with $\nu = 7.90$ Hz. Monotonically decreasing the amplitude value of the periodic signal, the transitions from triangular (T) \rightarrow irregular (I) \rightarrow elliptical (E) \rightarrow elliptical and rhombic (E*) \rightarrow square (S) \rightarrow circular (C) patterns were observed.

A_f (V)	Mode	Images
2.0	T	
1.8	T	
1.6	T	
1.4	T	
1.2	T	
1.0	T	
0.9	I	
0.7	I	
0.6	E	
0.5	E	
0.47	E	
0.44	E	
0.42	E	
0.4	E	
0.39	E	
0.38	E	
0.37	E*	
0.36	E*	
0.35	S	
0.3	S	
0.25	C	

for the corresponding points (a), (b), and (c) have been added to the Supplemental Material [54].

B. PSR: Irregular \rightarrow elliptical \rightarrow irregular patterns

In order to study the transition from irregular (I) \rightarrow regular (E) \rightarrow irregular (I) patterns, a pretreatment of the mercury drop was necessary (to observe a well-defined transition among the different patterns of the liquid metal in the presence of noise). This pretreatment protocol consisted of applying an external periodic square signal for 30 min (triangular mode, $A_f = 3.0$ V and irregular mode, $A_f = 0.85$ V, both with $\nu = 7.90$ Hz, 15 min each). To study the I \rightarrow E \rightarrow I

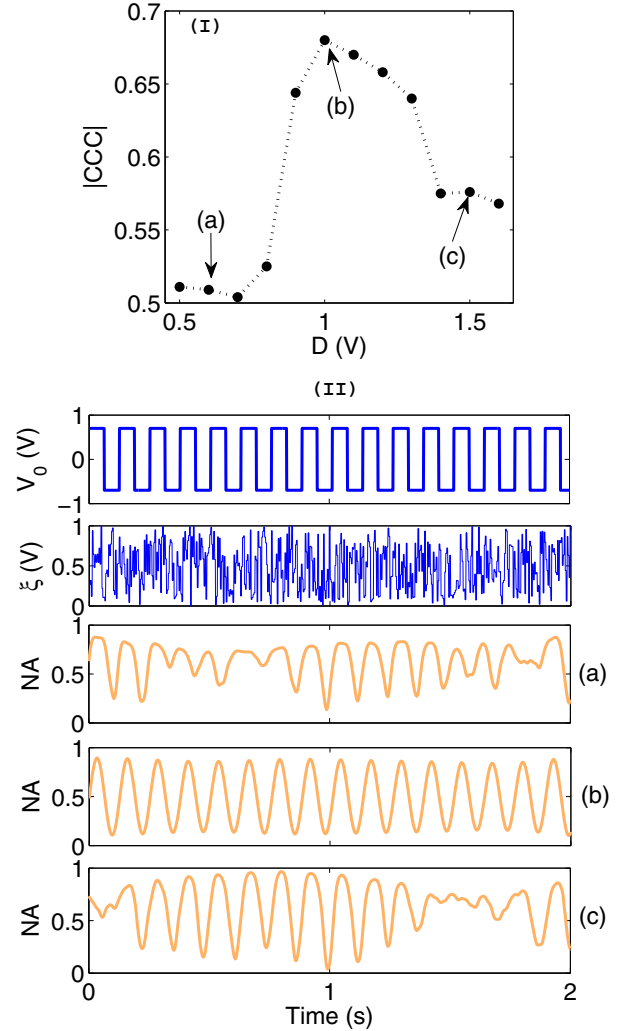


FIG. 2. (I) $|CCC|$ vs D . The points (a), (b), and (c) in the CCC curve correspond to the lower (0.6 V), optimum (1.0 V), and higher (1.5 V) values of the noise amplitude. (II) In blue (dark-gray) color, the upper panel shows the time series of the periodic subthreshold signal and the lower panel represents a biased white noise signal. The time series in orange (light-gray) color from (a) to (c) represent the mechanical activities (normalized area, NA) corresponding to the points shown in the CCC curve. The set point A_f was chosen to be 0.7 V and forcing frequency (ν) was 7.90 Hz.

pattern transitions, we selected the $A_f = 0.85$ V as the set-point amplitude for the periodic signal (irregular shape) and $\nu = 7.90$ Hz.

Figure 3(I) shows the unimodal curve for CCC. For the intermediate values region of D , CCC has higher values. In this region, the pattern exhibited by the liquid metal was the regular, elliptical mode. For the higher and lower values of D , the lower values of CCC indicate a lower correlation between the input and the output signals due to the irregular oscillations of the Hg drop.

The square-wave signal, blue (dark-gray) color, in the upper panel of Fig. 3(II), shows the time series of the applied periodic forcing and in the lower panel the blue (dark-gray) noisy time series represents the biased noise signal at $D = -1.0$ V. Figures 3(IIa)–3(IIc), in orange (light-gray) color

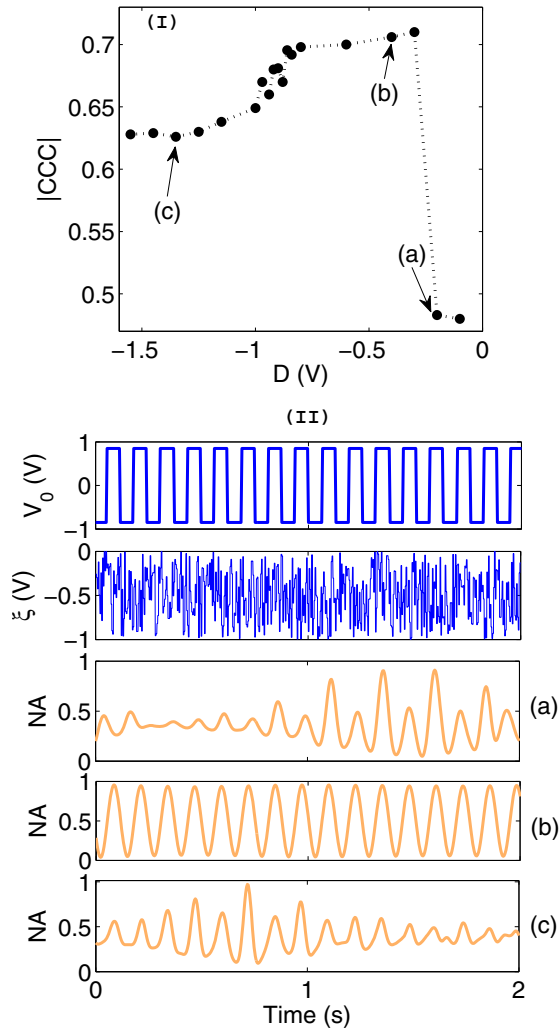


FIG. 3. (I) $|CCC|$ vs D . The points (a), (b), and (c) in the CCC curve correspond to the lower (-0.2 V), optimum (-0.4 V), and higher (-1.35 V) values of the noise amplitude (absolute values). (II) In blue (dark-gray) color, the upper panel shows the time series of the periodic subthreshold signal, the lower panel in blue (dark-gray) color, represents a biased white noise signal and the time series in orange (light-gray) color from (a) to (c) represent the normalized area (NA) time series of the mechanical activities corresponding to the points in the CCC curve. The set point A_f was chosen to be 0.85 V and ν was 7.90 Hz.

show a section of the NA time series (mechanical activities) of the liquid metal under the influence of stochastic perturbations. In Figs. 3(IIa) and 3(IIc), the time series correspond to the mechanical oscillations of the irregular patterns. In this

case, for higher values of noise amplitude, the liquid metal exhibited irregular patterns, i.e., a composition of elliptical, square, rhombic, rectangular, and circular shapes, which was not observed without noise (see Table I). The videos (Video2a, Video2b, and Video2c) for the points (a), (b), and (c) are in the Supplemental Material [54].

IV. SUMMARY AND DISCUSSION

Our results show that the liquid metal Hg exhibits regular and irregular patterns depending on the amplitude of the external periodic forcing. The selected pattern of the mercury drop was subsequently regulated under the influence of the white noise signal. The cross-correlation coefficient technique for the transitions from I (irregular) \rightarrow T (triangular) \rightarrow I (irregular) and I (irregular) \rightarrow E (elliptical) \rightarrow I (irregular) exhibits a unimodal profile for the curve, characteristic of stochastic resonance.

The reason for using biased noise is that the triangular shape of the liquid metal is at a higher energy level as compared to the elliptical shape. It implies that positive bias amplitude would help in the transition toward triangular shape whereas negative bias amplitude would assist in the transition toward elliptical shape. In our experiments, biased noise (positive and negative amplitudes) provides additional leverage, but the pattern transitions from I (irregular) \rightarrow T (triangular) \rightarrow I (irregular) and I (irregular) \rightarrow E (elliptical) \rightarrow I (irregular) shapes are not only because of bias. The complete pattern transitions from irregular \rightarrow regular (triangular or elliptical) \rightarrow irregular are possible only if we superimpose the biased noise on the subthreshold signal.

An electric field regulates the shape of the liquid metal. Manipulation and regulation of liquid metals using low potential differences is the cutting edge of energy-efficient liquid metal research. In our experimental results, the selection and regulation of liquid metal patterns by a white noise signal presents an insight into these studies. Along with the regulation of the patterns, we also observed the SR phenomenon using a liquid metal drop, which can be of further interest to the scientific community. Our experimental findings using an MBH system, a liquid metal, are reproducible and robust.

ACKNOWLEDGMENTS

Inputs from the members of the Experimental Non-linear Dynamics group at the Physics Department of IIT Bombay are immensely appreciated. Financial support from DST (India) (Project Reference No. EMR/2016/000275) and IIT Bombay is acknowledged.

- [1] C. B. Eaker and M. D. Dickey, *Appl. Phys. Rev.* **3**, 031103 (2016).
- [2] M. D. Dickey, *Adv. Mater.* **29**, 1606425 (2017).
- [3] G. Bo, L. Ren, X. Xu, Y. Du, and S. Dou, *Adv. Phys.: X* **3**, 1446359 (2018).
- [4] X. Yang, S. Tan, B. Yuan, and J. Liu, *Sci. China: Technol. Sci.* **59**, 597 (2016).
- [5] D. K. Verma, A. Q. Contractor, and P. Parmananda, *J. Phys. Chem. A* **117**, 267 (2013).
- [6] J. Olson, C. Ursenbach, V. I. Birss, and W. Laidlaw, *J. Phys. Chem.* **93**, 8258 (1989).
- [7] J. Lee and C.-J. Kim, *J. Microelectromech. Syst.* **9**, 171 (2000).
- [8] J. L. Ocampo-Espindola, E. Ramírez-Álvarez, F. Montoya, P. Parmananda, and M. Rivera, *J. Solid State Electrochem.* **19**, 3297 (2015).
- [9] Z. Yu, Y. Chen, F. F. Yun, D. Cortie, L. Jiang, and X. Wang, *Phys. Rev. Lett.* **121**, 024302 (2018).
- [10] G. Lippmann, *Ann. Phys. (NY)* **225**, 546 (1873).

- [11] J. Keizer, P. A. Rock, and S.-W. Lin, *J. Am. Chem. Soc.* **101**, 5637 (1979).
- [12] S. Castillo-Rojas, J. L. Gonzalez-Chavez, L. Vicente, and G. Burillo, *J. Phys. Chem. A* **105**, 8038 (2001).
- [13] D. K. Verma, H. Singh, A. Q. Contractor, and P. Parmananda, *J. Phys. Chem. A* **118**, 4647 (2014).
- [14] E. Ramírez-Álvarez, J. L. Ocampo-Espindola, F. Montoya, F. Yousif, F. Vázquez, and M. Rivera, *J. Phys. Chem. A* **118**, 10673 (2014).
- [15] S. Smolin and R. Imbihl, *J. Phys. Chem.* **100**, 19055 (1996).
- [16] P. Kumar and P. Parmananda, *Chaos* **28**, 045105 (2018).
- [17] A. Biswas, D. Das, and P. Parmananda, *Phys. Rev. E* **95**, 042202 (2017).
- [18] A. Zacharias and L. D. Smullin, *IRE Trans. Electron. Devices* **7**, 172 (1960).
- [19] A. A. Penzias and R. W. Wilson, *Astrophys. J.* **142**, 419 (1965).
- [20] W. C. Schmidt and J. C. Oliverio, *IEEE Trans. Ind. Gen. Appl.* **3**, 259 (1969).
- [21] R. Benzi, A. Sutera, and A. Vulpiani, *J. Phys. A: Math. Gen.* **14**, L453 (1981).
- [22] R. Benzi, G. Parisi, A. Sutera, and A. Vulpiani, *Tellus* **34**, 10 (1982).
- [23] C. Nicolis and G. Nicolis, *Tellus* **33**, 225 (1981).
- [24] K. Wiesenfeld and F. Moss, *Nature (London)* **373**, 33 (1995).
- [25] L. Gammaitoni, P. Hänggi, P. Jung, and F. Marchesoni, *Rev. Mod. Phys.* **70**, 223 (1998).
- [26] E. Sánchez, M. A. Matias, and V. Pérez-Muñuzuri, *Phys. Rev. E* **56**, 4068 (1997).
- [27] H. Nakao, K. Arai, and Y. Kawamura, *Phys. Rev. Lett.* **98**, 184101 (2007).
- [28] F. Flandoli, B. Gess, and M. Scheutzow, *Probab. Theory Relat. Fields* **168**, 511 (2017).
- [29] A. Longtin, A. Bulsara, and F. Moss, *Phys. Rev. Lett.* **67**, 656 (1991).
- [30] J. K. Douglass, L. Wilkens, E. Pantazelou, and F. Moss, *Nature (London)* **365**, 337 (1993).
- [31] P. Jung, U. Behn, E. Pantazelou, and F. Moss, *Phys. Rev. A* **46**, R1709 (1992).
- [32] D. F. Russell, L. A. Wilkens, and F. Moss, *Nature (London)* **402**, 291 (1999).
- [33] Gerardo J. Escalera Santos, M. Rivera, and P. Parmananda, *Phys. Rev. Lett.* **92**, 230601 (2004).
- [34] I. Tiwari, R. Phogat, P. Parmananda, J. L. Ocampo-Espindola, and M. Rivera, *Phys. Rev. E* **94**, 022210 (2016).
- [35] M. Nurujjaman, A. N. Sekar Iyengar, and P. Parmananda, *Phys. Rev. E* **78**, 026406 (2008).
- [36] A. Guderian, G. Dechert, K.-P. Zeyer, and F. Schneider, *J. Phys. Chem.* **100**, 4437 (1996).
- [37] A. S. Pikovsky and J. Kurths, *Phys. Rev. Lett.* **78**, 775 (1997).
- [38] G. Giacomelli, M. Giudici, S. Balle, and J. R. Tredicce, *Phys. Rev. Lett.* **84**, 3298 (2000).
- [39] B. Lindner and L. Schimansky-Geier, *Phys. Rev. E* **61**, 6103 (2000).
- [40] C. Y. Lee, W. Choi, J.-H. Han, and M. S. Strano, *Science* **329**, 1320 (2010).
- [41] S. Fauve and F. Heslot, *Phys. Lett. A* **97**, 5 (1983).
- [42] B. McNamara, K. Wiesenfeld, and R. Roy, *Phys. Rev. Lett.* **60**, 2626 (1988).
- [43] J. E. Levin and J. P. Miller, *Nature (London)* **380**, 165 (1996).
- [44] M. Perc, *Eur. Phys. J. B* **69**, 147 (2009).
- [45] H. Braun, M. Christl, S. Rahmstorf, A. Ganopolski, A. Mangini, C. Kubatzki, K. Roth, and B. Kromer, *Nature(London)* **438**, 208 (2005).
- [46] J. F. Lindner, B. K. Meadows, W. L. Ditto, M. E. Inchiosa, and A. R. Bulsara, *Phys. Rev. Lett.* **75**, 3 (1995).
- [47] T. Roy, S. Rumandla, V. Agarwal, and P. Parmananda, *J. Appl. Phys.* **122**, 124904 (2017).
- [48] Z. Gingl, L. B. Kiss, and F. Moss, *Europhys. Lett.* **29**, 191 (1995).
- [49] L. Gammaitoni, F. Marchesoni, E. Menichella-Saetta, and S. Santucci, *Phys. Rev. E* **49**, 4878 (1994).
- [50] A. R. Bulsara, A. Dari, W. L. Ditto, K. Murali, and S. Sinha, *Chem. Phys.* **375**, 424 (2010).
- [51] D. N. Guerra, A. R. Bulsara, W. L. Ditto, S. Sinha, K. Murali, and P. Mohanty, *Nano Lett.* **10**, 1168 (2010).
- [52] F. Moss, L. M. Ward, and W. G. Sannita, *Clin Neurophysiol* **115**, 267 (2004).
- [53] Y.-g. Leng, T.-y. Wang, Y. Guo, Y.-g. Xu, and S.-b. Fan, *Mech. Syst. Signal Process.* **21**, 138 (2007).
- [54] See Supplemental Material at <http://link.aps.org/supplemental/10.1103/PhysRevE.99.040201> for Video1a–Video1c and Video2a–Video2c. (a) Video1a, (b) Video1b, and (c) Video1c correspond to the noise amplitudes (a) 0.6 V, (b) 1.0 V, and (c) 1.5 V, respectively. (a) Video2a, (b) Video2b, and (c) Video2c correspond to the noise amplitudes (a) -0.2 V, (b) -0.4 V, and (c) -1.35 V, respectively.